Radiographic Facility in SINS Swierk

J. Bigolas, W. Drabik, E. Pławski ,A. Wysocka

Soltan Institute for Nuclear Studies, Swierk, Poland

Email contact of the main author: plawski@ipj.gov.pl

Abstract. In the paper the facility of 6 MeV linac electron accelerator is described. The accelerator can work in the electron mode and in the X-ray photon mode. Especially the photon beam may be used for radiographic non-destructive investigations on laboratory scale and after some modifications for industrial purposes. The design stages performed during the construction of the accelerator are described , examples of measurements and radiographic pictures are also presented.

1. Introduction

The radiographic facility build and tested in last two years in Accelerator Physics and Technology Department of SINS consists of electron accelerator and e-X conversion units placed in radiation shielded concrete room. The e-X conversion area is equipped additionally with 10cm lead shields surrounding the conversion head and exposure compartment . The electron accelerator is based on linear RF accelerating structure composed of 11 on axis coupled cells working in S band on the frequency 3 GHz. It is excited in the so called $\pi/2$ mode, the mode where the dimensional tolerances are strongly relaxed compare to standard π mode. Electrons are injected from thermionic diode gun pulsed together with RF power source exciting the accelerating structure.
The accelerated electron beam passes to air through thin (40 μm stainless steel) vacuum window. The water-cooled, removable e/X conversion head holding tungsten target can be placed few millimetres downstream this window. Thus, the facility can be used as operating in **electron beam mode** or **X ray beam mode** depending on demand.

2. The Design of the Accelerator

The basic components and parameters of accelerator are listed in TABLE I.

TABLE I: COMPONENTS AND PARAMETERS OF THE ACCELERATOR

Electron gun:
Diode, cylindrical Pierce geometry type, thermionic tungsten cathode, Energy/Intensity : 30keV/ 200mA in pulse 4 μsec ; variable repetition 50-300 Hz
RF accelerating structure:
11 cells, on axis coupled, $\pi/2$ mode, Resonant frequency: 2997.85 MHz ; Quality factor: 12 500 Nominal energy : 6 MeV ; Electron current : 100 mA in pulse, , 0.1 mA average Structure length (total) : 50 cm ; Working temperature 40 ± 1 °C
Beam Focusing :
Solenoid surrounding the accelerating structure Maximum attainable axial magnetic field 700 Gs . Magnetic quadrupole dublet on structure output Beam position correctors: two pairs of small coils underneath solenoid coil
e/X conversion unit (tungsten target) - radiographic parameters:
Electron beam energy: 6 MeV ; Focal spot: 2 mm max.; X-ray dose rate: 500 R/min/m Flaw detectability: 0.4%

2.1 Design Calculations and Optimisation

The construction of accelerator was preceded by thorough computational optimisation of electron gun and successive RF accelerating structure. The computational DC[1] and RF[2] codes, checked by beam dynamics codes developed in our Institute were used to get the optimum shapes of structures.

The samples of final computational results are presented in FIG.1, FIG. 2, FIG. 3 .

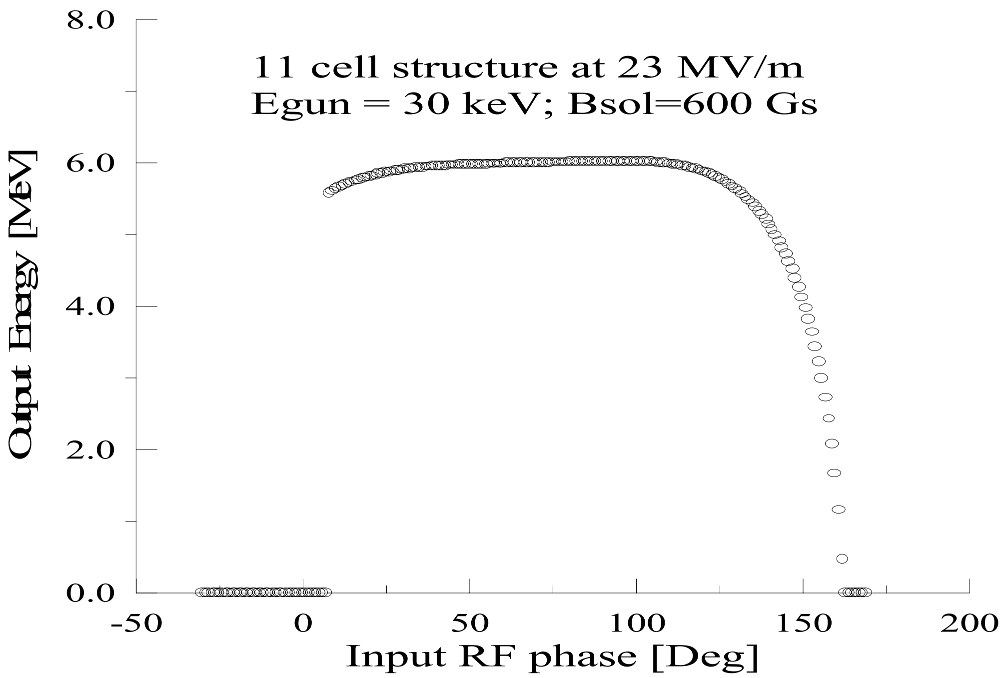

FIG. 1 Computed phase acceptance of accelerating structure.
23 MV/m amplitude corresponds to 15 MV/m mean field.

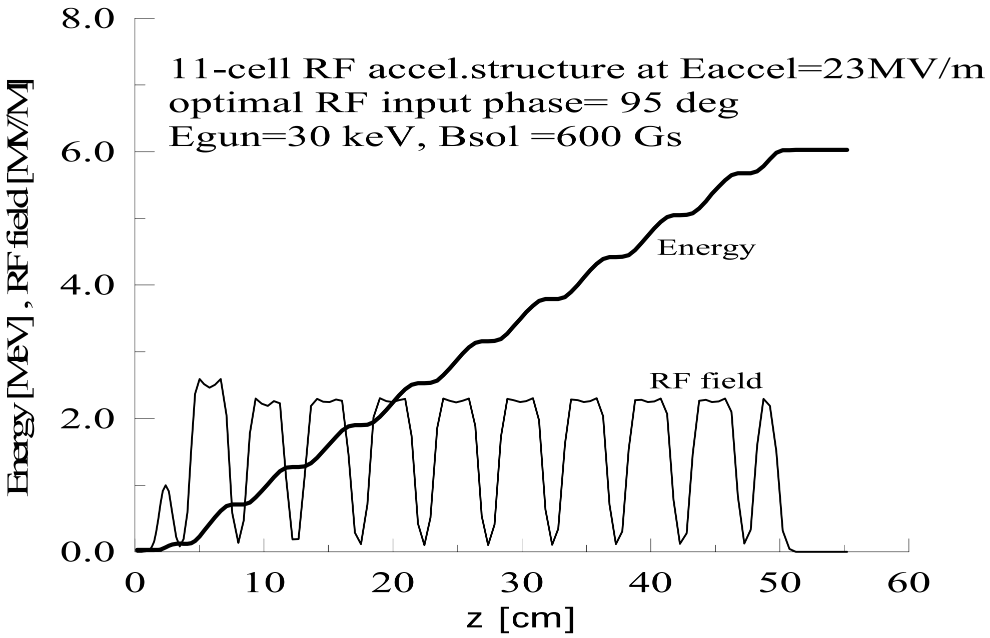

FIG. 2 Electron beam transmission through RF accelerating structure at optimal input phase 95^0 RF.

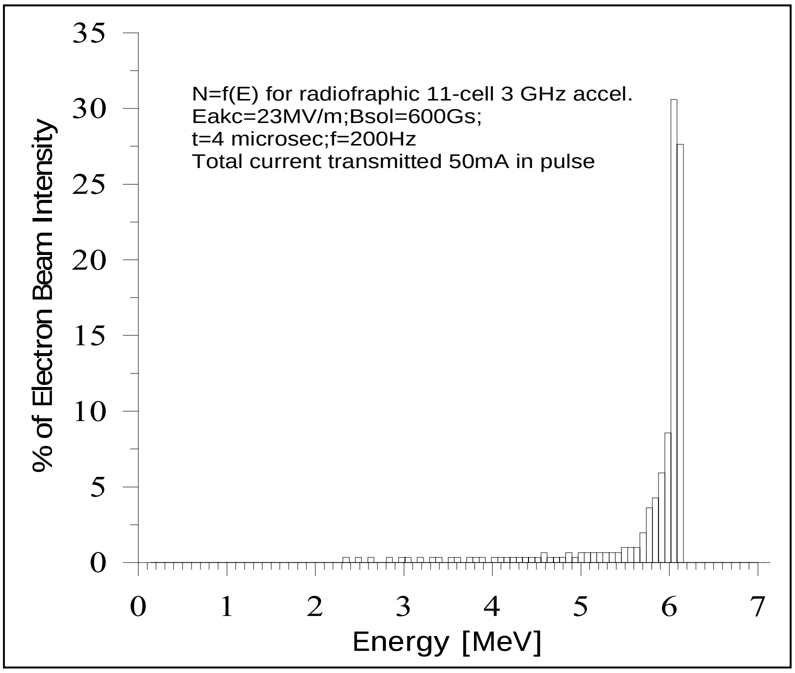

FIG. 3. Calculated electron energy spectrum on W target of radiographic 6 MeV accelerator. Beam diameter on target 2mm. Target thickness/diameter 1mm/10mm

2.2 RF Accelerating Structure and Auxiliaries

The components of RF accelerating structures are fabricated from certified OFHC copper. The guarantied Cu content is better than 99.995% and oxygen content below 1.0 ppm. This last number is extremely important if technology of brazing in hydrogen atmosphere is used. We have two options available: brazing in vacuum or brazing in hydrogen atmosphere . In the first case the grain size of copper is most critical while in the second the content of oxygen is very important. The structure actually mounted in radiographic facility was brazed in vacuum oven.
After the last brazing operation the whole structure is finally tuned to the working $\pi/2$ mode. The Slater perturbation method is applied with metal perturbing bead moved on axis.
Block diagram of the structure is shown in Fig.4.
RF power exciting electromagnetic field in accelerating structure is generated by 2999 MHz, 2 MW in pulse magnetron is delivered to coupling window to accelerating structure via pressurised WR284 waveguide system comprising , 4 -way circulator, RF power loads and various RF sensing and regulation devices shown in Fig.4. Automatic frequency tuning (AFC) system tunes the magnetron to the structure frequency.

The photograph of accelerator with its RF , vacuum and cooling systems is shown in Fig.5

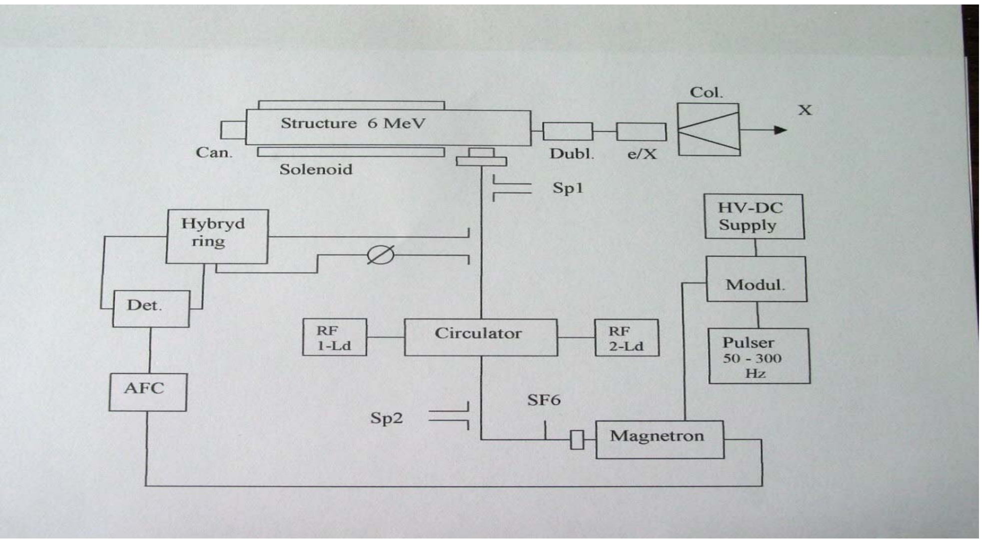

FIG. 4. Schematic layout of radiographic facility.

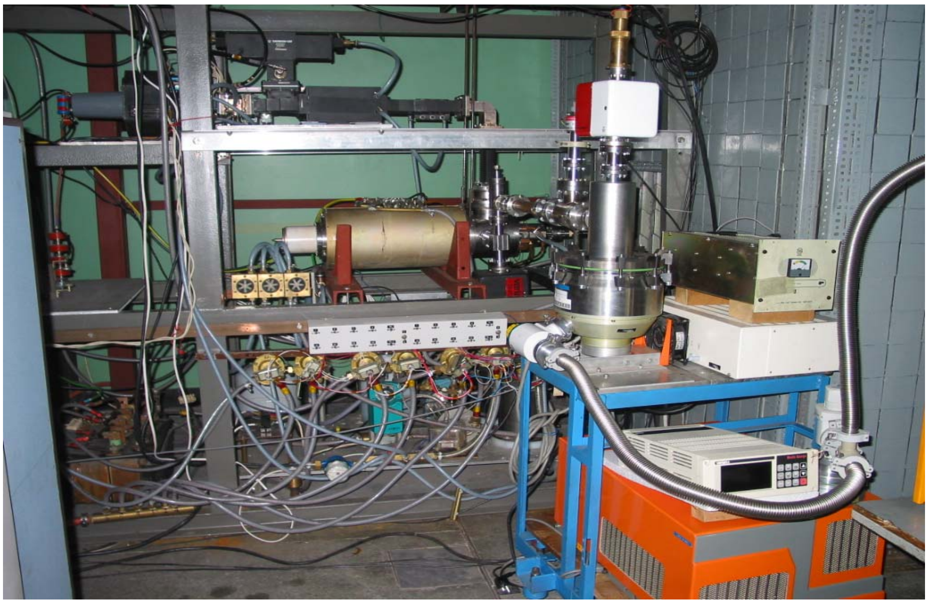

FIG. 5. 6 MeV electron linac mounted in shielded bunker

2.3 Electron Beam Spectra Measurements

In the electron mode the measurements of electron beam spectra were made using simple magnetic analyser. The electron beam emerging form the accelerating structure is deflected in magnetic field of analyser by 60 degrees and after passing through energy defining slit is collected in the Faraday cup. The current of the Faraday cup is converted to the voltage signal and measured with the oscilloscope. The electron beam energy was determined from relationship between magnetic field intensity and energy. The result was verified by calculations of electron beam trajectories in the magnetic gap taking into account fringe effects .

In the Fig.6 the shape of the spectrum is drawn for magnetron parameter Um=4 VA and electron beam Ie= 6 mA in 4 microsec pulse.

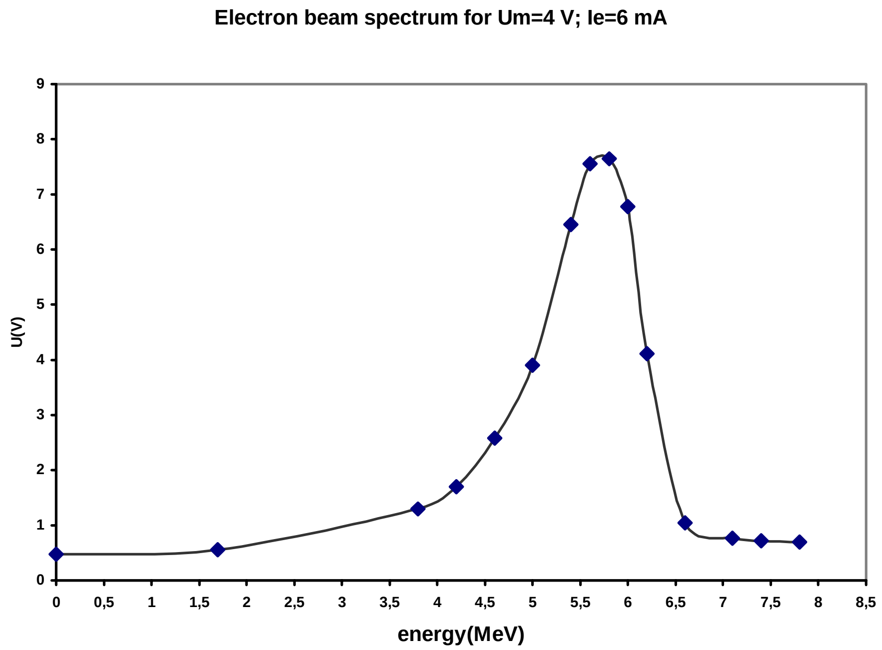

FIG. 6. The measured electron energy spectrum of radiographic accelerator

Afterwards, electron beam spectra were used as the input data for e_/X ray Monte Carlo calculations.

3. Monte Carlo Calculations of the Photon Beam

The Monte Carlo code BEAMnrc/EGSnrc[3] , was used to calculate spectral distribution, mean energy distribution and fluence versus position for a photon beam in the radiographic accelerator.

Calculations were done for 7 x 10^7 particles, using electron transport cutoff ECUT=0.7 MeV, and photon transport cutoff PCUT=0.01 MeV. For the maximum fractional electron energy loss per step (ESTEPE), a value of 0.25 was used. Relativistic spin effects have been icluded in nuclear elastic scattering for accurate calculations near high Z interfaces. The electron step algorithm PRESTA-II (an essential requirement for accurate high–Z interface simulations) and the exact boundary crossing algorithm BCA PRESTA-I were implemented.

A “Parallel Circular Beam with 2-D Gaussian X-Y Distribution” was used as the source type of incident electron beam in the BEAMnrc code. The value of FWHM of the Gaussian distribution was set to 2 mm. The energy spectrum of the electron beam was set from 2.3 to 6.25 MeV. A Tungsten target of 6mm diameter and 1 mm thickness was put as the e^-/X conversion unit.

The influence of different energy spectra of electrons was investigated.

Phase space files (PHSP) were generated for scoring planes at different distances from the tungsten target. PHSP contains data relating to particle position, direction, charge, etc. for every particle crossing a scoring plane. The BEAMDP program was used for processing phase space files and to derive spectral distribution, mean energy distribution and fluence versus position of a photon beam in air. Figures 7 and 8 show the energy spectrum and the fluence versus position of a photon beam for the field area with a radius of 10 cm at a distance of 100 cm from the tungsten target. Photon fluence is normalised by the energy bin width, number of incident particles and the area of the field being considered. The mean energy of photon beam changes were from 1.18 MV to 1.14 MV at a distance of 10 cm from the beam axis.

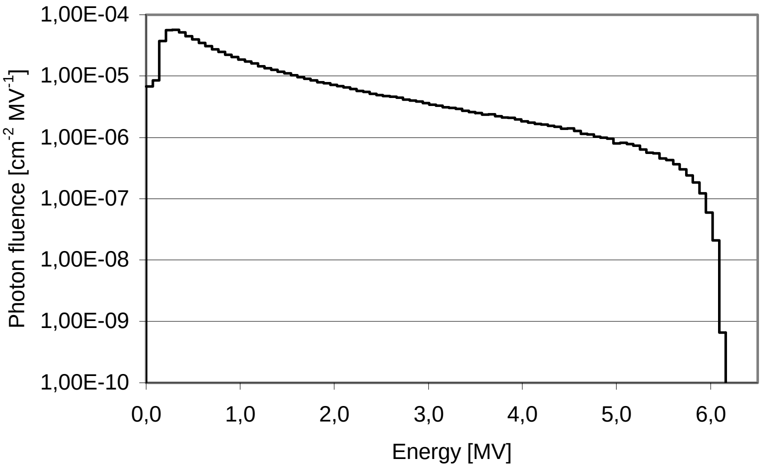

FIG. 7. Energy spectrum of a photon beam in air for the field area with a radius of 10 cm at a distance of 100 cm from the tungsten target.

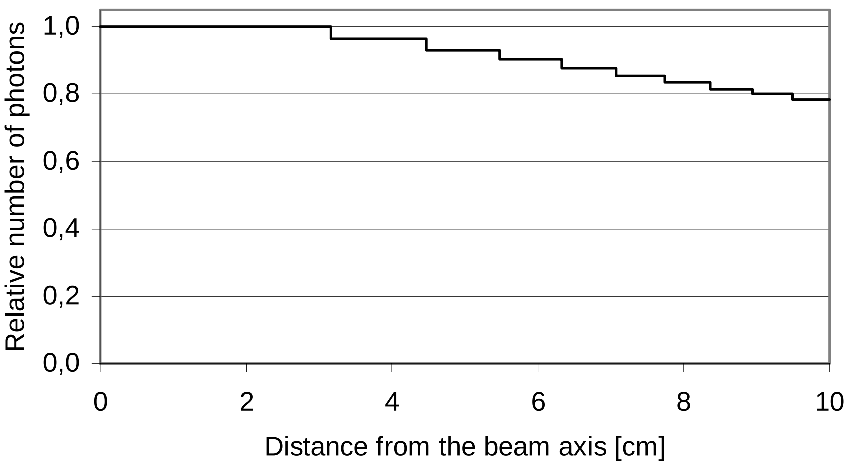

FIG. 8. Fluence versus position of a photon beam in air for the field area with a radius of 10 cm at a distance of 100 cm from the tungsten target.

4. The Radiographic Pictures

The Kodak Industrex AA 400 film was chosen for taking the radiographic images and experiments with different expositions and filters were performed to obtain the good radiographic contrast.
The radiographic images of two different specimens are presented below (Figs 9 and 10)

FIG.9. Radiographic image of the diode electron gun

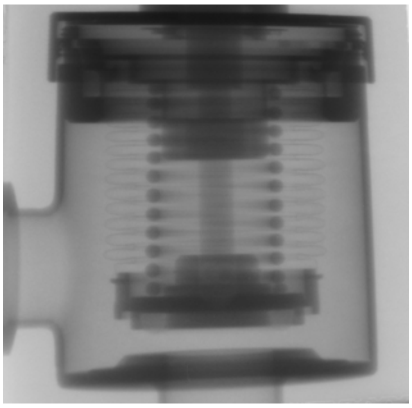

FIG. 10. Radiographic image of the vacuum valve

[1] W.B. Herrmansfeld, “E-Gun Code”, SLAC – 331/1988 Report
[2] J.H. Billen, L.M. Young, “Poisson-Superfish” Los Alamos LA-ur-96-1834 Report
[3] I.Kawrakow and D.W. O. Rogers “The EGSnrc Code System: Monte Carlo Simulation of Electron and Photon Transport”, *National Research Council of Canada Report* PIRS-701, (2001)